

A DESCRIPTION OF THE MICROSTRUCTURE AND THE MICROMECHANICAL PROPERTIES OF SPRUCE WOOD

ZDENĚK PROŠEK^{a,*}, VLASTIMIL KRÁLÍK^a, JAROSLAV TOPIČ^a,
VÁCLAV NEŽERKA^a, KATEŘINA INDROVÁ^{a,b}, PAVEL TESÁREK^{a,b}

^a Faculty of Civil Engineering, Czech Technical University in Prague, Thákurova 7, 166 27 Prague, Czech Republic

^b Institute of Physics, Academy of Sciences of the Czech Republic, Cukrovarnická 10, 162 00 Prague, Czech Republic

* corresponding author: zdenek.prosek@fsv.cvut.cz

ABSTRACT. Knowledge about the microstructure and the morphology of individual phases within wood tissues is essential for numerous applications in materials engineering and in the construction industry. The purpose of the work presented here is to monitor the distribution of elastic stiffness within the tissues of individual cells using state-of-art equipment and exploiting emerging methods, such as modulus mapping, to investigate the morphology of the individual phases. Quasi-static nanoindentation was carried out on cell walls of spruce earlywood and latewood tracheids to obtain values for the indentation modulus, which is closely related to the Young modulus of the material. Dynamic modulus mapping, also known as nanoDMA, was utilized to obtain a map of the elastic moduli over the entire tracheid cross-section. In particular, it was found that the indentation stiffness of the cells walls ranges between 10.5 GPa for of earlywood tracheids and 12.5 GPa for latewood tracheids. The difference between the elastic stiffness of earlywood and latewood is attributed to the different chemical composition and the orientation of the fibrils. The data that has been acquired is indispensable for micromechanical modeling and for the design of engineered products with superior mechanical properties.

KEYWORDS: Norway spruce, atomic force microscopy, optical microscopy, nanoindentation, nanoDMA.

1. INTRODUCTION

About 76 % of the afforested area in the Czech Republic comprises coniferous trees, and more than one half of these are spruces. This is reflected in the construction industry, where spruce is the most widely-used timber. For this reason, we focused our study on spruce wood tissues from Norway spruce, which is the only species of spruce and the most commonly encountered tree in Europe.

Wood in general is a non-homogeneous and highly anisotropic material at sub-micro-, micro- and macro-level. The microstructure and the micromechanical properties have a significant influence on the macroscopic properties of timber.

1.1. MICROSTRUCTURE OF WOOD CELLS

Coniferous trees were present on Earth before the first deciduous trees emerged, and their structure is therefore simple and very regular. Only two kinds of wood cells can be found in them, tracheids and parenchymal cells. The parenchymal cells create medullary rays and are involved in the construction of resin channels.

On the other hand, the longitudinally extending tracheids, comprising up to 95 % of the total wood volume, are the basic structural tissue. Their cell structure is closed and oblong, with a rectangular up to hexagonal cross-section. Their length varies from 2 to 6 mm, and their width is usually in the range between 0.02 and 0.1 mm. Two basic types of

tracheids can be found in wood - earlywood tracheids and latewood tracheids [1].

Earlywood tracheids are formed at the beginning of the growing season, and their purpose is to deliver water and dissolved nutrients up the tree. For this reason, earlywood tracheids are thin-walled, with a cell wall thickness of about 2 to 3 μm , and they have a relatively big internal cavity for better conduction [2]. Latewood tracheids are formed in the second half of the growing season, and their main function is to reinforce the tree trunk against mechanical loading. Latewood tracheids have a thick wall, about 7 μm in thickness, and the internal cavity is significantly smaller than in the case of earlywood cells.

About 7 % of the wood volume consists of parenchymal cells in the shape of short prisms. They are maintained for a variously limited period, and are located in the sapwood region. Their function is to deliver and store starch and nutrients for some period in the sapwood at the periphery of the tree trunk. In addition, these cells are responsible for the formation of medullary rays, consisting of resin channels and of parenchymal cells oriented perpendicular to the longitudinal axis of the trunk and the annual rings. After the parenchymal cells die, they can retain water or stay empty.

The resin channels are formed by disintegration or spreading of the cell walls between neighboring parenchymal cells, so the long resin channels are sur-

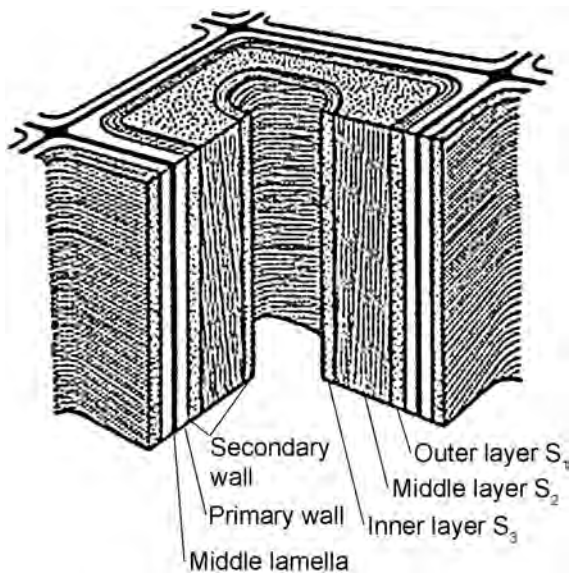


FIGURE 1. Scheme of the wood cell tissues (reproduced from [2]).

rounded by parenchymal cells. When the tree suffers a surface wound, resin is transported to the damaged part to provide a seal.

A comprehensive study of the structure of cell walls in the wood tissues by means of electron microscopy revealed that the walls are composed of multiple layers, each composed of millions of fibrils. The different properties of the individual layers are caused by the arrangement of the chemical properties of the fibrils [3].

In the direction from the perimeter to its center, a wood cell is composed of the middle lamella, then a primary wall, then a secondary wall composed of three layers, and a cavity called the lumen (see Figure 1). The middle lamella is thin, ranging in thickness between 0.1 and 0.3 μm , and its chemical and physical properties are similar to the properties of the primary wall. The middle lamella is usually well connected with the primary wall, so it is sometimes referred to as a part of the composite lamella consisting of the middle lamella and neighboring cell walls [2]. However, the structure of the composite lamella can easily be separated by chemical agents into individual anatomic elements [1].

The thickness of the primary wall does not differ from the thickness of the wall of the middle lamella; it is about 0.05 to 0.2 μm in thickness. It has an irregular arrangement of the fibrils, and is oriented in an angle ranging from 0 to 90° with respect to the longitudinal cell axis. It is assumed that the fibrils connect the primary layer and the middle lamella, thus forming a firm connection [3].

Before electron microscopy was available, Bailey and Kerr [4] used iodine staining and polarization microscopy to find that the secondary wall is composed of three layers, commonly referred to as outer (S_1), middle (S_2) and inner (S_3) (Figure 1). While investigating the cell cross-section they found that the

outer and inner layers are brighter than the middle layer, due to the different orientation of the fibrils in the individual layers.

The outer layer of the secondary cell wall is composed of four lamellas, and it is usually 0.1 to 0.4 μm in thickness. In this layer, the fibrils are arranged in two perpendicular directions at an angle of about 60° with respect to the longitudinal axis of the cell [3].

The middle layer of the secondary wall forms the major part of the wood cells, and it is therefore the most important component from the mechanical point of view. It is composed of 30 to 150 lamellas, and the fibrils are arranged at an angle of 10° with respect to the longitudinal axis of the wood cell. The middle layer has a superior influence on the properties of the wood cells and consequently of the entire tree trunk. The properties of the middle layer have an impact on the anisotropy, shrinkage, strength and ductility of the wood.

The inner layer of the secondary wall is similar to the inner layer, except that the orthogonal fibrils are arranged at an angle of between 60° and 90° with respect to the longitudinal axis of the cell [3].

1.2. MICROMECHANICAL PROPERTIES OF WOOD

Knowledge of micromechanical properties is crucial for understanding the micromechanics of wood that are responsible for the macromechanical properties of timber. Information about the microstructure and the micromechanical properties of individual tissues can be efficiently used for developing wood-based engineering products such as fiberboard and wood-plastic composites [5]. Two techniques are commonly used in experimental investigations of mechanical properties at micro-level: tensile tests of individual fibers, and nanoindentation.

The famous English engineer, A. A. Griffith, did pioneering work on determining the tensile strength of a single fiber [6]; his first tests on glass fiber were carried out in 1921. A significant simplification of these tests was achieved in 1938 with the invention of strain gauges. Further research on single wood fibers 0.5 to 30 mm in length and ranging between 15 and 40 μm in diameter was conducted in 1959 by Jayne [7]. It turned out that the most problematic issue is how to attachment the fibers firmly to the clamps of the testing machine. After several unsuccessful trials using adhesives, the fibers were finally clamped using abrasive paper. Since then, numerous methods have been developed for the purposes of testing single fibers in tension. In 1971, Page [8] designed a frame to which the fibers are attached with the use of two glass plates that are connected to the frame. This invention achieved popularity, and the method has also been used for testing other materials, e.g. metals and paper [5].

Nanoindentation was developed in 1992 by Oliver and Pharr [9], and within a short time it became

Reference	Indentation modulus [GPa]	MFA [°]
Latewood		
Wimmer [10]	21 ± 3.34	—
Wimmer [11]	15.81 ± 1.61	3
Gindl [14]	17	0
Gindl [14]	18	0
Gindl [12]	15.34	5
Gindl [15]	17.08	5
Konnerth [16]	20	0
Transitionwood		
Wimmer[10]	21.27 ± 3	—
Gindl [13]	16.1	—
Gindl [14]	16	20
Gindl [12]	13.46	7.5
Gindl [15]	17.54	7
Konnerth [16]	17	9
Konnerth [16]	16.8	11.5
Earlywood		
Wimmer [10]	13.49 ± 5.75	—
Gindl [14]	11.5	35
Gindl [14]	8	50
Konnerth [16]	12.5	17.5

TABLE 1. Indentation modulus and micro-fibril angle (MFA) of the secondary cell wall layer S_2 determined by nanoindentation on Norway spruce [10–16].

the most popular method for investigating micromechanical properties on various materials. Wimmer et al. [10] utilized nanoindentation in 1997 to investigate the mechanical properties of wood cells, and published information for the first time about the stiffness of spruce earlywood, latewood and transition wood. His results are summarized in Table 1, and are compared with the results provided by other authors. Wagner et al. [17] found the relationship between indentation depth and the results that they obtained, and established a depth of 200 to 250 nm as optimal for obtaining the most accurate results. Indentation depth is not the only factor influencing the results, which are also affected by lignin content and by the angle of the fibrils in the cell wall. Jäger et al. [18] found the relation between the angles of the fibrils on the nanoindentation results, and they came to the conclusion that the indentation modulus and hardness are proportional to the number of fibrils in the cell wall. Attempts were made to measure the micromechanical properties of the outer secondary wall S_1 , but these failed because the results were influenced by the surrounding layers. For this reason, all successful nanoindentation measurements have been conducted on the middle secondary wall S_2 .

1.3. AIM OF THE PAPER

The main purpose the work presented here was to provide detailed information about the distribution of the elastic stiffness within the cross-section of earlywood and latewood cells. The biggest obstacle appeared to be the preparation of the samples, especially due to enormous sensitivity to the moisture of wood tissue. The paper provides comprehensive information about the individual phases, which is needed for micromechanical modeling and homogenization. The necessary comprehensive information was not available from the literature, so the data that we obtained has had to be discussed very carefully and compared with the findings of other authors.

Modulus mapping is emerging as an advanced method for monitoring the field of elastic stiffness over a selected area. This method, based on dynamic measurements in a raster located at predetermined point on the material, has been successfully used for micromechanical analyses e.g. of bio-materials [19], and the results are in agreement with the data obtained by quasi-static indentation. However, no applications of this method for monitoring the distribution of elastic stiffness over a cross-section of wood tissues has been reported in the available literature.

2. EXPERIMENTAL METHODS

2.1. OPTICAL AND ELECTRON MICROSCOPY

Microscopy images were acquired using a NEOPHOT 21 optical metallurgy microscope with up to 1k magnification capabilities, and a PHILIPS XL-30 scanning electron microscope that uses a thin ray of electrons to scan the selected surface area. The scanning electron microscope requires a detector to track the reflected electrons and digitally reproduce and record the surface texture. Various detectors based on signals provided by the reflected electrons have been used for our purposes. In particular, we used a detector of secondary electrons, a detector of reflected electrons, and a gaseous detector of secondary electrons [20].

2.2. ATOMIC FORCE MICROSCOPY

Atomic Force Microscopy (AFM) utilizes a scanning probe that moves close to the investigated surface in order to capture the variations of atomic forces on a predetermined raster measured by means of piezoelectric transducers. The method has become extensively used, e.g. for investigating thin layers [21]. The probe tip size is usually at the scale of μm , with a radius of about 10 nm [22].

AFM microscopy was performed on the DME 2329 DS 95-200 Dual ScopeTM Probe Scanner. Within this study, we used the non-contact mode of the AFM, which is based on the observation that van der Waals forces (of the magnitude of 10^{-12} N) decrease the resonance frequency of the cantilever. These forces are strongest from 1 to 10 nm above the surface of the sample. In oscillation mode, we detect the changes

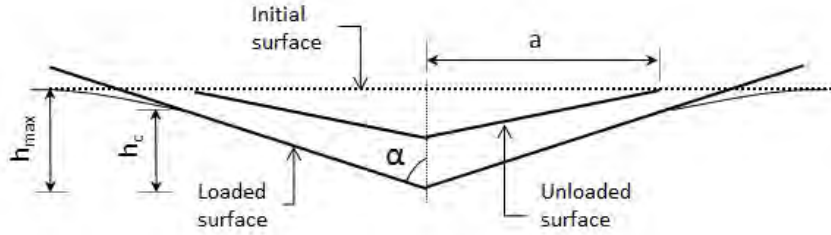


FIGURE 2. Scheme of the indentation with an indication of the depth at full loading and after unloading (reproduced from [9]).

in the amplitude of the cantilever oscillation caused by changes in the distance between the probe and the sample. The topographic image is thus constructed without any contamination or damage to the sample.

The size of the scanned raster was equal to 65×65 microns, and the scanning time was limited to 2 minutes to avoid excessive heating of the device. The vertical resolution (measurement range) was set to 0.5 nm.

2.3. STATIC NANOINDENTATION

The static indentation method is widely used nowadays, and is a very popular experimental technique for measuring the elastic stiffness and hardness on various materials, usually metals, glass, ceramics and thin coatings. This type of measurement can be performed on a very small volume, so it is suitable for investigating composite materials at microscale.

The principle is based on imprinting a micrometer-sized diamond tip into the investigated material and recording the loading force and the indentation depth. In most of the measurements, the indentation depth is of the order of hundreds of nanometers. Various nanoindentation tips are available, e.g. spherical or Berkovich tips, and several techniques are used to ensure that the analysis also provides information about the plastic hardening, the yield stress or the viscosity of the material [23].

Standard processing of the measured data is based on the assumption of a perfectly homogeneous isotropic material in the volume affected by the indentation, and the elastic and non-elastic material parameters are usually derived from the nanoindentation data, using an analytic solution. When there are distinct phases, however, the indentation results can provide information about individual inclusions and the interfaces between them. The pioneering work of Hertz (1882) [24] dealt with the imprint of an elastic tip in a homogeneous medium. Sneddon (1965) [25] derived an analytical relationship between the loading force, the depth of an imprint and the contact area for individual indentation tips.

A typical output from nanoindentation measurements consists of two elastic constants: the hardness parameter and the elastic stiffness. The hardness parameter (H) is defined as the mean of the contact

pressure at maximum loading force P_{max} :

$$H = \frac{P_{max}}{A}, \quad (1)$$

where A is the contact indentation tip area.

During the loading process, the indented material deforms both in the elastic range and in the plastic range. The plastic response on the load-displacement curve is eliminated during unloading, allowing the user to determine the local material stiffness, known as the reduced modulus E_r . The value for the reduced modulus can therefore be obtained from the unloading part of the recorded force-displacement diagram from the tangent $(dP/dh)|_{P_{max}}$, normalized by the contact area:

$$E_r = \frac{\sqrt{\pi}dP}{2\sqrt{A}dh}. \quad (2)$$

Knowing the stiffness of indenter tip E_i , the true indentation modulus of the measured material can be expressed, using the Hertz solution for a contact of two compliant bodies, as

$$\frac{1}{E_r} = \frac{1 - \nu^2}{E} + \frac{1 - \nu_i^2}{E_i}, \quad (3)$$

where ν and ν_i are the values of the Poisson ratio representing the tested material and the indenter, respectively. The solution of Oliver and Pharr [9], which is most commonly used for an analysis of experimentally obtained nanoindentation data, suggests a formula for the contact depth in the following form:

$$h_c = h_{max} - \varepsilon \frac{P_{max}}{\frac{dP}{dh}}, \quad (4)$$

with constant ε dependent on the indentation tip geometry, e.g. $\varepsilon = 0.726$ in the case of a Berkovich tip and $\varepsilon = 0.750$ if a spherical tip is used. It should be noted that if a non-symmetric tip is used, Equation (1) must be rendered by a geometric correction parameter β , so that

$$E_r = \frac{\sqrt{\pi}dP}{2\beta\sqrt{A}dh}. \quad (5)$$

For a Berkovich tip, the β parameter is established as 1.034.

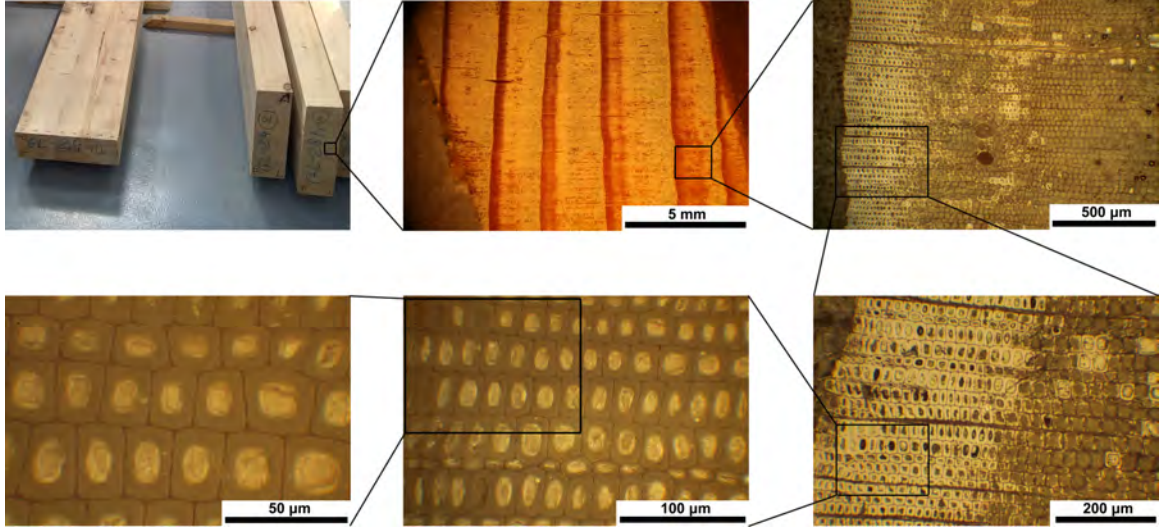


FIGURE 4. Microstructural hierarchy of wood tissues.

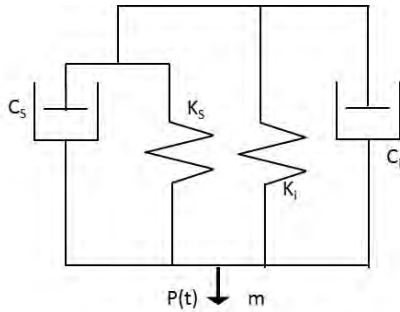


FIGURE 3. A dynamic model of the indenter and the tested specimen (reproduced from [26]).

2.4. DYNAMIC NANOINDENTATION

The dynamic method (nanoDMA) assumes a dynamic model of the indenter and the test sample with a single degree of freedom. The model parameters include indenter mass m , sample stiffness K_s , and damping coefficient C_s , as well as the indenter stiffness and damping coefficient K_i and C_i , respectively (see Figure 3).

In addition, the damping coefficient, representing the air gap in the displacement sensor C_i , the contact stiffness K_s , and the stiffness of the leaf spring holding the indenter shaft, K_i , should also be taken into account in the model. The frame stiffness is usually large enough to be considered infinite.

When using the dynamic nanoDMA method, a dynamically applied harmonic force $P(t) = P_0 \sin \omega t$ with amplitude P_0 and frequency $f = \omega/2\pi$ is superimposed on a quasi-static load P_{max} . The equation of motion for the indenter tip can be expressed as

$$m\ddot{h} + C\dot{h} + Kh = P_0 \sin \omega t. \quad (6)$$

The solution to the above equation is a steady-state displacement oscillation at the same frequency as the excitation:

$$h = h_0 \sin(\omega t - \phi), \quad (7)$$

where h_0 is the deformation amplitude and ϕ represents the deformation phase shift with respect to the excitation force. The amplitude and the phase shift can be used to calculate the contact stiffness, using the dynamic model described in Figure 3, assuming the following formulas for the deformation amplitude and the phase shift [26]:

$$h_0 = \frac{P_0}{\sqrt{(K_s + K_i - m\omega^2)^2 + ((C_i + C_s)\omega)^2}}, \quad (8)$$

$$\phi = \tan^{-1} \frac{(C_i + C_s)\omega}{K_s + K_i - m\omega^2}. \quad (9)$$

Knowing the stiffness and the damping of the sample, the viscoelastic properties can be determined using the values of the reduced storage modulus, E'_r and the loss modulus, E''_r to determine the ratio between the loss and storage moduli, $\tan \delta = E''_r/E'_r$, according to the following formulas:

$$E'_r = \frac{K_s \sqrt{\pi}}{2\sqrt{A}}, \quad E''_r = \frac{\omega C_s \sqrt{\pi}}{2\sqrt{A}}, \quad (10)$$

$$\tan \delta = \frac{E''_r}{E'_r} = \frac{\omega C_s}{K_s}, \quad (11)$$

where A is the contact area obtained from the quasi-static calibration for the particular contact depth. The storage and loss moduli of the sample can be determined using the same relationship as in Equation (5), which is used when interpreting the data from quasi-static indentation. The storage modulus depends on the elastic recovery of the sample, which is expressed in terms of the recovered energy after one loading cycle. The loss modulus corresponds to the damping of the material, and depends on the time delay between reaching the maximum force and the maximum deformation. The ratio of the loss and storage moduli ($\tan \delta$) is then related to the material viscosity, independent of the contact area.

The instrumentation used in our study could combine nanoDMA with the imaging capabilities of *in-situ*

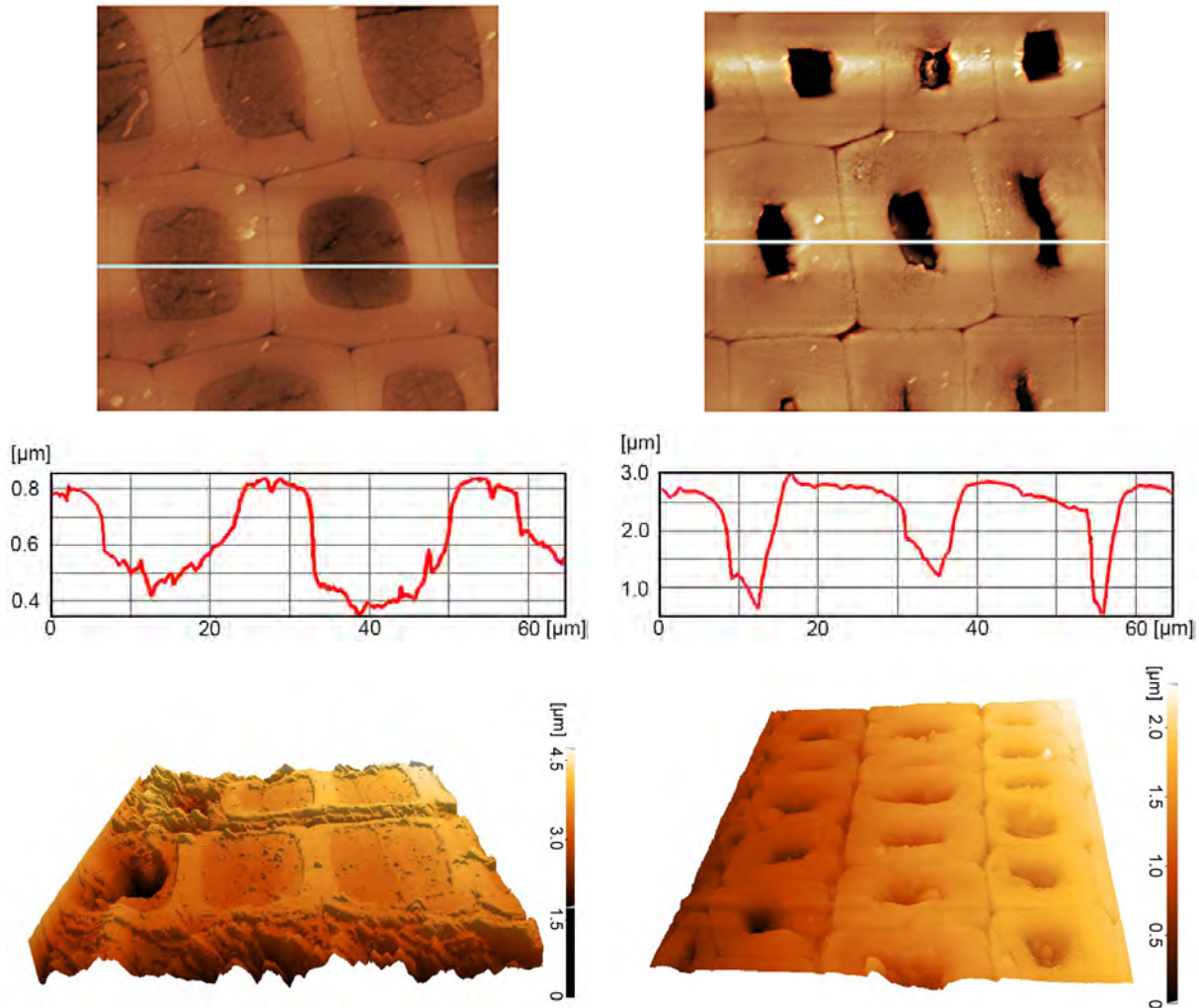


FIGURE 5. AFM images of an earlywood cross-section (left) and a latewood cross-section (right), $65 \times 65 \mu\text{m}$.

imaging, meaning that nanoDMA can be extended to a larger area. During the monitoring process, the system continuously records the storage and loss moduli of the sample as a function of the position on the measured surface. This raster measurement provides information about the stiffness variation and the morphology of the sample surface. This type of approach, which extends the nanoDMA method, is referred to as modulus mapping [27].

3. PREPARING THE SAMPLES

3.1. TESTED SAMPLES

The spruce wood samples used for the investigation and for testing were extracted from a glue laminated timber beam (GLT) composed of 30×200 mm lamellae of length equal to 1.5 m. This wood must be dried to a moisture content ranging between 8% and 15% in order to prevent swelling and consequent cracking or failure of the glue due to excessive water content. For this purpose, the timber was artificially dried using hot air drying kilns with controlled air humidity. After reaching the required moisture, the timber lamellae

were gradually cooled down and the timber beams were stored in heated warehouses for several days.

3.2. SAMPLE PREPARATION

The samples of wood with a cross section of 10×10 mm, were cut in the required directions with respect to the grain, and were sealed with Struers Epofix Kit epoxy resin. After the resin had hardened, the samples were sliced, ground, and polished with silica papers to achieve the best possible quality of the sample surface, going from grit of 800 grains/cm² to grit of 4000 grains/cm². The whole grinding process was carried out under water, using an electronic device. Polishing was performed using an emulsion containing 0.25 micron nanodiamonds for 15 minutes. After each step, the sample was cleaned in an ultrasonic bath of distilled water.

4. RESULTS AND DISCUSSION

4.1. MICROSTRUCTURE

The microstructure of the samples was investigated by means of optical microscopy, electron scanning microscopy and AFM. The earlywood portion of an

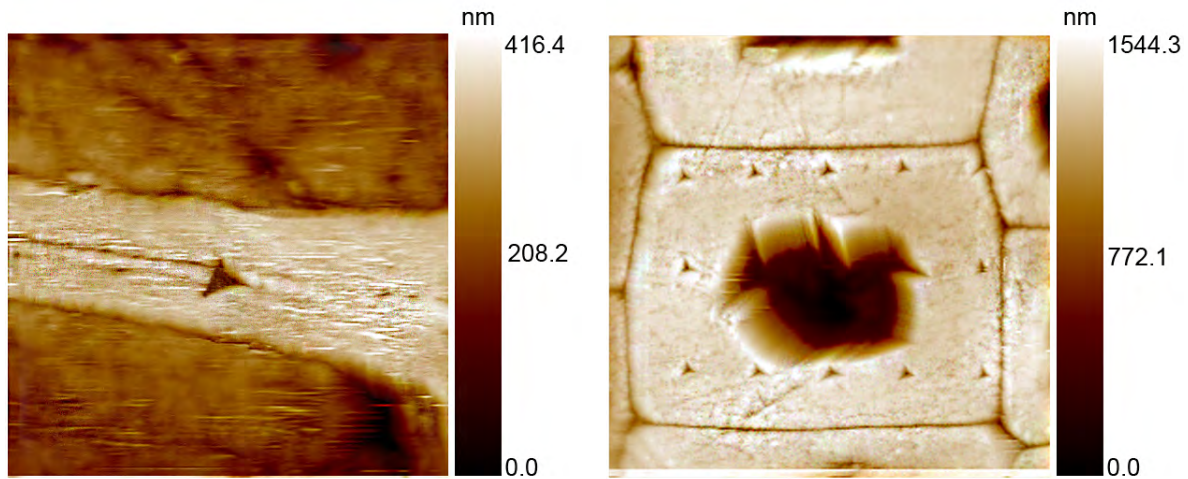


FIGURE 6. Matrix of indents in an earlywood cell wall, $18.55 \times 18.55 \mu\text{m}$ (left) and in a latewood cell wall, $50 \times 50 \mu\text{m}$ (right).

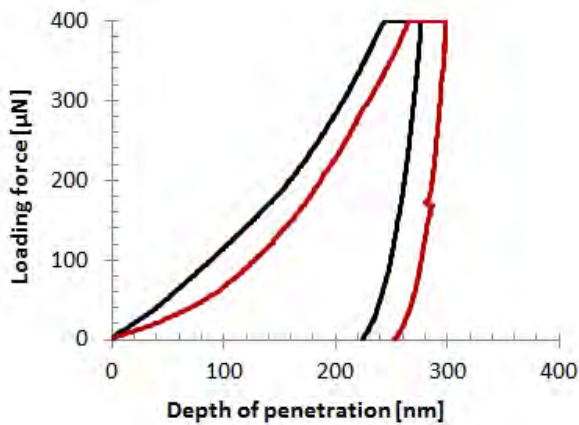


FIGURE 7. Load-displacement diagram obtained by nanoindentation on the cell wall of earlywood.

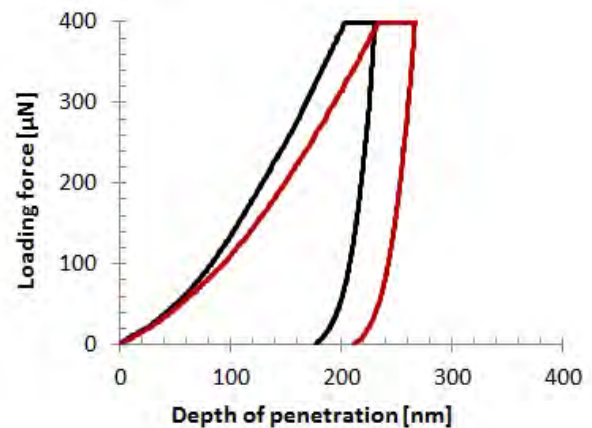


FIGURE 8. Load-displacement diagram obtained by nanoindentation on the cell wall of latewood.

annual ring was 0.79 mm in thickness, and the latewood cells were arranged in a region 1.14 mm in thickness. The visible microcracks within the samples had formed due to the artificial drying applied in the initial stage of GLT processing. The first method was accomplished using a NEOPHOT 21 microscope (Figure 4) to acquire basic information about the microstructure. AFM was used for the analysis in order to obtain a detailed description of individual phases within the cells of the spruce samples (Figure 5).

Optical microscopy revealed a honeycomb-like structure of hexagonally-shaped tracheids with an average size of $30 \mu\text{m}$ (earlywood) or $41 \mu\text{m}$ (latewood) in the tangential direction (T) with respect to the annual rings, and an average size of $27 \mu\text{m}$ (earlywood) or $32 \mu\text{m}$ (latewood) in the radial direction (R). The wall of the earlywood tracheids was significantly thinner, as demonstrated in Figure 5, with a cell wall thickness of about $2 \mu\text{m}$ (T) and $3 \mu\text{m}$ (R), and a lumen of $18 \mu\text{m}$ (R) and $17 \mu\text{m}$ (T) to provide nutrient transport. The latewood cells of significantly higher density and with

thicker walls, $12 \mu\text{m}$ (R) and $7 \mu\text{m}$ (T), contained a smaller lumen with an average size of $19 \mu\text{m}$ (R) and $13 \mu\text{m}$ (T), in order to perform as a reinforcement against the mechanical loading.

4.2. MICROMECHANICAL PROPERTIES

4.2.1. STATIC INDENTATION

Both the earlywood and the latewood wood cells were indented in various cell regions, using a Berkovich tip, in order to obtain a map of the micromechanical properties. The standard indentation loading function was pursued, consisting of a constant loading stage (5 seconds), a holding period (8 seconds) and an unloading stage (5 seconds). The maximum loading capacity of the indenter was $400 \mu\text{N}$. Figure 6 shows a 4×5 indentation matrix captured during in-situ monitoring, using the Hysitron Tribolab[®] scanning device. In order to prevent any interaction between individual indents, their minimum spacing was set to $3 \mu\text{m}$.

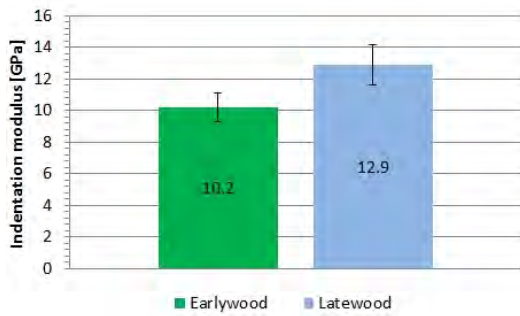


FIGURE 9. Measured indentation modulus, with an indication of the standard deviations.

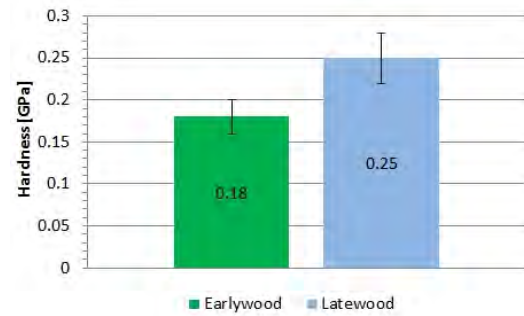


FIGURE 10. Measured indentation hardness, with an indication of the standard deviations.

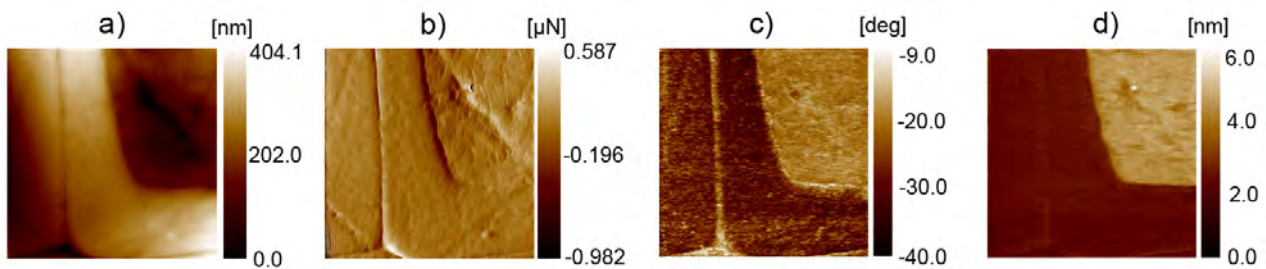


FIGURE 11. Topography, gradient, amplitude and phase shift, determined by DMA on a $16 \times 16 \mu\text{m}$ earlywood tracheid area.

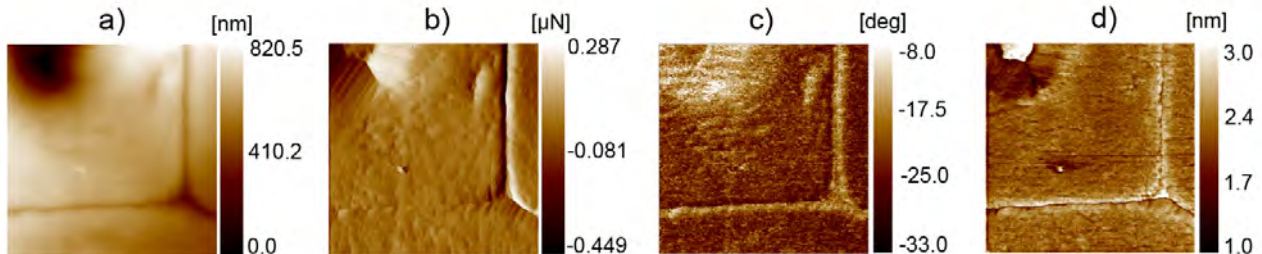


FIGURE 12. Topography, gradient, amplitude and phase shift determined by DMA on a $16 \times 16 \mu\text{m}$ latewood tracheid area.

The chosen nanoindentation load-displacement diagrams, reaching minimum and maximum indentation depth, are plotted in Figures 7 and 8. The average contact depth was equal to 270 nm for earlywood cells and 222 nm for latewood cells. This depth is satisfactory for the surface roughness (Figure 5) and small enough to prevent the influence of the limited wall thickness (Figure 6). The mean deviation of the surface roughness of the tested samples was lower than 20 nm.

The Oliver and Pharr [9] method was used to evaluate the elastic parameters from the experimentally obtained data. The mean values for indentation modulus and hardness with an indication of the standard deviation are presented in Figures 9 and 10. These results are in agreement with the data published by other authors [10–16].

4.2.2. MICROMECHANICAL PROPERTIES – NANODMA INDENTATION

For the modulus mapping method, the dynamic force was harmonically superimposed (with amplitude 5 μN and frequency 150 Hz) on the nominal quasi-static contact force 12 μN . The measurements were performed over an area of $16 \times 16 \mu\text{m}$. The amplitude and the phase shift recorded in the raster obtained from the DMA measurements are presented in Figures 11 and 12, which also document the morphology of the sample. Since there was negligible viscosity, as indicated by the relatively small magnitude of the measured loss moduli, the values for the storage moduli can be considered as the reduced elastic stiffness modulus, obtained by means of a quasi-brittle nanoindentation test.

Figures 13 and 14 present the storage modulus

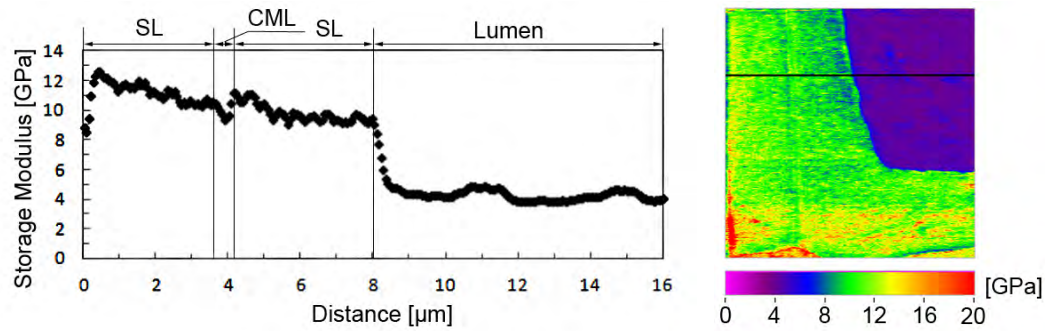


FIGURE 13. Earlywood storage modulus map, $16 \times 16 \mu\text{m}$ (left) and a line-plot projection to a horizontal section: SL – secondary wall, CML – composite middle lamella (right).

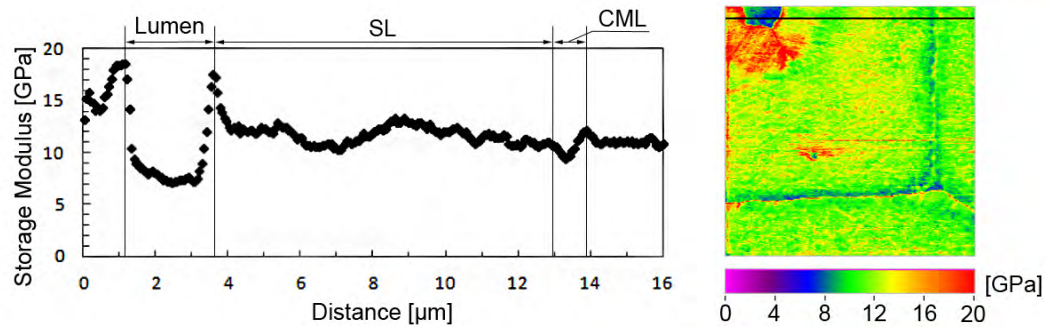


FIGURE 14. Latewood storage modulus map, $16 \times 16 \mu\text{m}$ (left) and a line-plot projection to a horizontal section: SL – secondary wall, CML – composite middle lamella (right).

	Static indentation		DMA indentation	
	Indentation modulus [GPa]	st. d.	Indentation modulus [GPa]	st. d.
Earlywood	10.2	0.9	10.4	1.4
Latewood	12.9	1.3	12.09	2.06

TABLE 2. Indentation modulus of tracheid walls; st. d. represents standard deviation of the measured data.

mapping, representing the earlywood and latewood samples. It can be observed that the cell walls exhibit greater elastic stiffness than the lumen area and the composite middle lamella (the middle lamella and the primary wall). However, the cell walls contain significant local deviations. The mean indentation modulus of the secondary cell wall tissue (denoted SL in Figures 13 and 14) was established as 10.4 ± 1.4 GPa for the earlywood tracheids, and 12.09 ± 2.06 GPa for the latewood tracheids. Irrespective of the tissue, the composite middle lamella (denoted by CML in Figures 13 and 14) exhibited stiffness equal to 9.45 ± 0.19 GPa.

4.3. DISCUSSION

All the results obtained by means of static indentation and the modulus mapping method are summarized in Table 2. The values seem reasonable for the effective properties of spruce wood, as published in the literature [10–16]. Static indentation could not be performed on the middle lamella because of its limited size.

The difference between the elastic stiffness of the earlywood and latewood cell walls is attributed to the different chemical composition and the angle of the fibrils. The earlywood cells contain more lignin and less cellulose, resulting in reduced elastic stiffness. The same effect can also be observed for the middle lamella, which contains twice as much lignin as the latewood cell walls, and less than one third of the amount of cellulose. Moreover, the fibrils are not systematically arranged, so the stiffness of the middle lamella is 2.64 GPa lower than the stiffness of the latewood cell walls. The work of Gindl et al. [14], which focused on the micromechanical properties of individual phases in the wood tissues, suggests that lignin, which bonds to hemicellulose, does not have any significant impact on the hardness parameter, and influences only the elastic stiffness value. The minor discrepancy between our quasi-static nanoindentation results for the latewood cells and the results of other authors may be due to the angle of the fibrils deposited in the cell walls.

The influence of the orientation angle of the fibrils

on the elastic stiffness was investigated by Jäger et al. [18], who found a clear correlation between these quantities. According to their equation describing the relationship between the orientation of the fibrils and the indentation modulus, the fibrils of earlywood cell walls in our samples were oriented at an angle of 39.5° and, in the case of latewood, at an angle of 23.5°. These values are larger than we had expected on the basis of a literature study, which had indicated angles of about 10°. The large values may be due to defects in the vicinity of the extracted samples, or due to the way the samples were prepared.

According to Gindl et al. [15], the compressed wood defect increases the angle of the fibrils up to 50°, while Wagner et al. [17] found that polishing the samples can also increase the angle.

5. CONCLUSION

The results of our study provide detailed information about the morphology and the elastic stiffness of individual phases in wood from Norway spruce. The quasi-static nanoindentation and dynamic modulus mapping method have provided valuable data about the distribution of stiffness within individual earlywood and latewood cells. The data contributes to our basic understanding of the wood microstructure, and can also be efficiently used for analytical or numerical homogenization and micromechanical modeling. On the basis of our findings, it can be followed that:

- microcracking cannot be avoided if the wood is dried using elevated temperatures exceeding 100 °C,
- the use of quasi-static nanoindentation and nanoDMA can provide detailed information about the distribution of the elastic stiffness within a single spruce tracheid,
- the indentation modulus of tracheid cell walls is equal to 10.3 GPa for earlywood and 12.5 GPa for latewood,
- the difference between the mechanical properties of earlywood and latewood is caused by the different chemical composition, by the lignin content at the expense of cellulose, and by the different orientation of the fibrils,
- the influence of fibrils and chemical composition is clearly demonstrated in the case of the middle lamella, which has an indentation modulus about 2.64 GPa lower than that for latewood cell walls,
- earlywood fibrils are inclined by about 39.5°, while latewood fibrils are oriented at an angle of 23.5°.

Future research will be focused on an investigation of the angle of the fibrils, using optical microscopy and X-ray diffraction. The data will be correlated with the elastic stiffness of the investigated phases, and the knowledge that is acquired will be used for upscaling the elastic stiffness using micromechanical modeling [28]. The model will be validated with the

use of macroscopic testing by means of the impulse excitation method, which has been successfully exploited by Kuklík et al. [29] for investigating timber elements.

ACKNOWLEDGEMENTS

Financial support from the Faculty of Civil Engineering, Czech Technical University in Prague (SGS projects SGS14/122/OHK1/2T/11 and SGS14/121/OHK1/2T/11). The authors also thank the Center for Nanotechnology in Civil Engineering at the Faculty of Civil Engineering, CTU in Prague, and the Joint Laboratory of Polymer Nanofiber Technologies of the Institute of Physics, Academy of Science of the Czech Republic, and the Faculty of Civil Engineering, CTU in Prague.

REFERENCES

- [1] Gandelová, L., Horáček, P. and Šlezingerová, J.: *Nauka o dřevě*. Brno, Mendelova zemědělská a lesnická univerzita v Brně, 2002, p. 1–176.
- [2] Balabán, K.: *Anatomie dřeva*. Praha, SZN, 1955, p. 1–216.
- [3] Kettunen, P. O.: *Wood structure and properties*. Tampere, Trans tech publication, 2006, p. 1–401.
- [4] Bailey, I. W. and Kerr, T.: The visible structure of the secondary wall and its significance in physical and chemical investigations of tracheary cells and fibers. *Protoplasma*, vol. 26, 1935, p. 273–300. DOI:10.1007/BF01628654
- [5] Eder, M. et al.: Experimental micromechanical characterisation of wood cell walls. *Wood Science and Technology*, vol. 47, 2013, p. 163–182. DOI:10.1007/s00226-012-0515-6
- [6] Griffith, A. A.: The phenomena of rupture and flow in solids. *Philos Trans R Soc Lond*, vol. 221, 1921, p. 163–198.
- [7] Jayne, B. A.: Mechanical properties of wood fibers. *Tappi*, vol. 42, 1959, p. 461–467.
- [8] Page, D. H., El-Hosseiny, F. and Winkler, K.: Behaviour of single wood fibres under axial tensile strain. *Nature*, vol. 229, 1971, p. 252–253. DOI:10.1038/229252a0
- [9] Oliver, W. C. and Pharr G. M.: An improved technique for determining hardness and elastic-modulus using load and displacement sensing indentation experiments. *J Mater Res*, vol. 7, 1992, p. 1564–1583. DOI:10.1557/JMR.1992.1564
- [10] Wimmer, R. et al.: Longitudinal hardness and elastic stiffness of spruce tracheid secondary walls using nanoindentation technique. *Wood Science and Technology*, vol. 31, 1997, p. 31–141. DOI:10.1007/BF00705928
- [11] Wimmer, R. and Lucas, B. N.: Comparing mechanical properties of secondary wall and cell corner middle lamella in spruce wood. *IAWA*, vol. 18, 1997, p. 77–88.
- [12] Gindl, W., Gupta, H. S. and Gunwald, C.: Lignification of spruce tracheid secondary cell walls related to longitudinal hardness and modulus of elasticity using nano-indentation. *Canadian Journal of Botany*, Vol. 80, 2002, p. 1029–1033. DOI:10.1139/b02-091

- [13] Gindl, W. and Gupta, H. S.: Cell-wall hardness and elastic stiffness of melamine-modified spruce wood by nano-indentation. *Composites*, vol. 33, 2002, p. 1141–1145. DOI:10.1016/S1359-835X(02)00080-5
- [14] Gindl, W. et al.: Mechanical properties of spruce wood cell walls by nanoindentation. *Appl Phys*, vol. 79, 2004, p. 2069–2073. DOI:10.1007/s00339-004-2864-y
- [15] Gindl, W. and Schöberl, T.: The significance of the elastic modulus of wood cell walls obtained from nanoindentation measurements. *Composites*, vol. 35, 2004, p. 1345–1349. DOI:10.1016/j.compositesa.2004.04.002
- [16] Konnerth, J. et al.: Actual versus apparent within cell wall variability of nanoindentation results from wood cell walls related to cellulose microfibril angle. *J Mater Sci*, vol. 44, 2009, p. 4399–4406. DOI:10.1007/s10853-009-3665-7
- [17] Wagner, L., Bader, T. K. and Borst, K.: Nanoindentation of wood cell walls: effects of sample preparation and indentation protocol. *J Mater Sci*, vol. 49, 2009, p. 94–102. DOI:10.1007/s10853-013-7680-3
- [18] Jäger, A. et al.: The relation between indentation modulus, microfibril angle, and elastic properties of wood cell walls. *Composites*, vol. 42, 2011, p. 677–685. DOI:10.1016/j.compositesa.2011.02.007
- [19] Jiroušek, O. et al.: Use of modulus mapping technique to investigate cross-sectional material properties of extracted single human trabeculae. *Chemické listy*, vol. 106, 2011, p. 442–445.
- [20] Ekertová, L. and Frank, L.: *Metody analýzy povrchů – Elektronová mikroskopie a difrakce*. ACADEMIA, 2003.
- [21] Siegel, J. and Kotál, V.: Preparation of Thin Metal Layers on Polymers. *Acta Polytechnica*, vol. 47, 2007, p. 9–11.
- [22] Binnig, G., Quate, C. F. and Gerber, Ch.: Atomic force microscope. *Phys. Rev. Lett.*, vol. 56, 1986, p. 930–935. DOI:10.1103/PhysRevLett.56.930
- [23] Fisher-Cripps, A.C.: *Nanoindentation*. New York, Springer Verlag, 2002, p. 1–163.
- [24] Hertz, H.: *Verhandlungen des Vereins zur Beförderung des Gewerbe Fleisses*. Macmillan & Co, London, vol. 64, 1882.
- [25] Sneddon, I. N.: The relation between load and penetration in the axisymmetric boussinesq problem for a punch of arbitrary profile. *International Journal of Engineering Science*, vol. 3, 1965, p. 47–57. DOI:10.1016/0020-7225(65)90019-4
- [26] Syed Asif, S.A, Wahl, K. J. and Colton, R. J.: Nanoindentation and contact stiffness measurement using force modulation with a capacitive load-displacement transducer. *Review of Scientific Instruments*, vol. 70, 1999, p. 2408–2414. DOI:10.1063/1.1149769
- [27] Syed Asif, S. A. et al.: Quantitative imaging of nanoscale mechanical properties using hybrid nanoindentation and force modulation. *Journal of Applied Physics*, vol. 90, 2001, p. 1994–2000. DOI:10.1063/1.1380218
- [28] Mishnaevsky L. and Qing H.: Micromechanical modelling of mechanical behaviour and strength of wood: State-of-the-art review. *Computational Materials Science*, vol. 44, 2008, p. 363–370. DOI:10.1016/j.commatsci.2008.03.043
- [29] Kuklík, P. and Kuklíková, A.: Nondestructive Strength Grading of Structural Timber. *Acta Polytechnica*, vol. 40, 2000.